



Published in final edited form as:

Adv Exp Med Biol. 2011 ; 716: 91–106. doi:10.1007/978-1-4419-9533-9_6.

Spatio-temporal Signaling in Mast Cells

Bridget S. Wilson^{*}, Janet M. Oliver, and Diane S. Lidke

Department of Pathology, University of New Mexico, Albuquerque, NM 87131

Abstract

This chapter summarizes the evidence for localized signaling domains in mast cells and basophils, with a particular focus on the high affinity IgE receptor, FcεRI, and its crosstalk with other membrane proteins. It is noteworthy that a literature spanning 30 years established the FcεRI as a model receptor for studying activation-induced changes in receptor diffusion and lipid raft association. Now a combination of high resolution microscopy methods, including immunoelectron microscopy and sophisticated fluorescence-based techniques, provide new insight into the nanoscale spatial and temporal aspects of receptor topography on the mast cell plasma membrane. Physical crosslinking of FcεRI with multivalent ligands leads to formation of IgE receptor clusters, termed “signaling patches,” that recruit downstream signaling molecules. However, classes of receptors that engage solely with monovalent ligands can also form distinctive signaling patches. The dynamic relationships between receptor diffusion, aggregation state, clustering, signal initiation and signal strength are discussed in the context of these recent findings.

Keywords

IgE receptor; FcεRI; rafts; microdomains

Introduction

Engagement of the high affinity IgE receptor, FcεRI, is the principal physiological stimulus for mast cell degranulation. This tetrameric receptor is composed of the IgE-binding α subunit, two γ subunits and a tetraspan β subunit. There are a total of three ITAMs (immunoreceptor tyrosine-based activation motifs), one in the carboxy terminus of the β subunit and one in each of the paired γ subunits. Activation occurs when IgE binds to polyvalent antigens, crosslinking a minimum of two FcεRI-IgE complexes thereby initiating a tyrosine kinase cascade that triggers histamine release and *de novo* synthesis of leukotrienes, prostaglandins¹ and an impressive list of cytokines and chemokines.² Biochemical details of this cascade have been the subject of many reviews, including Gilfillan and Rivera³ and other chapters in this volume.

In the 25 yr period spanning from 1975–2000, the FcεRI was the subject of pioneering studies that measured the mobility and behavior of membrane proteins. Emerging biophysical techniques, such as fluorescence recovery after photobleaching (FRAP), post-field relaxation after in situ electromigration and time-resolved phosphorescence anisotropy, were used to arrive at estimates of lateral diffusion rates of $1.5\text{--}4 \times 10^{-10}$ cm²/s for resting receptors.^{4,5} Rotational correlation values ranged from 23–65 ms^{6–8}, with slower values attributable to measurements at low temperatures. In these early studies, incomplete recovery from photobleaching was already recognized as an indication that a small fraction

^{*}To whom correspondence should be addressed: bwilson@salud.unm.edu.

of receptors were immobile in resting cells, with marked increases in the immobile fraction after antibody-mediated crosslinking and the concomitant observation of microaggregates and patches visible in the fluorescence microscope.^{4,9} Rotational mobility was also markedly restricted after receptor crosslinking.¹⁰ These and related studies led to a number of important hypotheses that are still being vigorously tested today. These include revision of classical Brownian diffusion models of cell membrane proteins to explain restricted lateral mobility¹¹ and the widely-held concept that FcεRI immobilization must be necessary for signal initiation.^{12,13} Antigen valency and structure, particularly as it relates to the orientation and distance of FcεRI subunits within aggregates, also continues to be a highly relevant topic¹⁴ that is strongly linked to both receptor immobilization and signaling efficiency.

Microdomains, Rafts and Islands

For almost forty years, the fluid mosaic model has provided a conceptual framework for plasma membrane structure.¹⁵ This model, which integrated many studies from the preceding decade, viewed cellular membranes as two-dimensional solutions composed of integral membrane proteins within a lipid matrix. It proposed that most membrane constituents diffuse rapidly and are randomly arranged, but it acknowledged the possibility of ordered membrane regions based on early EM images of clustered proteins. Variations of this model arose however, beginning with the terms “lipid rafts” and “liquid ordered and disordered domains”.^{16–18} Seminal studies by several groups working in the mast cell field provided compelling evidence for the lipid raft hypothesis, based in large part upon the recovery of FcεRI and its signaling partners or regulators in light fractions of sucrose gradients after stimulation.^{19–22} While the popularity of the lipid raft concept energized the membrane biology community, artifacts associated with merging of compartments by detergent treatment may have also led to misconceptions. This is now the prevailing view in the field, as evidenced by recent reviews stressing the heterogeneity of the membrane and the likelihood that microdomains are both small, readily exchangeable and complex.^{23–26} Clearly, more sophisticated and direct measurements are needed to both refine and correct this model.

An alternative view has re-emerged for membrane organization, referred to as the “protein islands” model.^{27,28} It is similar to the predictions of Yechiel and Edidin,²⁹ who proposed that “plasma membranes are organized into protein-rich lipid domains, separated by a protein-poor lipid continuum.” Importantly, the protein islands model explains membrane heterogeneity, based upon the strong segregation of distinct protein subpopulations with islands, and acknowledges rich association with cholesterol and cytoskeletal elements. The model revives appreciation for the influence of local protein density on diffusivity³⁰, a concept that is reinforced by evidence that protein-rich confinement zones transiently trap diffusing membrane proteins on T cells.³¹

Electron Microscopy Provides a Bird’s Eye View of FcεRI Signaling Patches

Scanning electron microscopy (SEM) provided the first nanoscale resolution images of immuno-gold labeled FcεRI “patches”,³² that were hinted at in the early immunofluorescence experiments.⁴ The size of patches, and the time course for their formation, was shown by SEM to be dependent on antigen dose.³³ By 2000, our group had developed the technology to prepare native membrane sheets ripped from rat basophilic leukemia (RBL-2H3) cells at various stages of activation.³⁴ With the improved resolution of transmission electron microscopy (TEM), these preparations could be labeled more efficiently by smaller nanogold particles and by other novel nanoparticles such as quantum

dots.³⁵ The sheets also permitted access to the cytoplasmic face of the membrane for labeling intracellular proteins recruited during signaling.

Figure 1 provides typical views of FcεRI signaling patches before (1A) and after 2 min stimulation with antigens with different valency (1B,C). Cells in Figure 1B were activated with DNP₂₄-BSA (0.1 μg/ml) while cells in Figure 1C were stimulated with a PEG-based flexible trivalent DNP ligand (10 nM). Note that, even in the resting state, receptors are not completely random (Fig 1A). Small clusters, ranging from 2–5 receptors, are typically found in addition to singlets. FcεRI clusters generally increase in size after antigen-mediated crosslinking,³³ although the increase is somewhat smaller in response to ligands of low valency or even with low concentrations of polyvalent antigens.³⁶ However, comparison of secretory responses for the two antigen conditions illustrated here (60–70% for DNP₂₄-BSA versus 10–30% for the PEG-trivalent ligand) makes it clear that *cluster size does not predict signaling output*.

To further drive this point home, crosslinking with a panel of divalent antibodies against the FcεRI α subunit yielded similar, small cluster sizes.³⁷ Importantly, only the signaling-competent antibodies showed dissociation from Lyn and recruitment of significant amounts of Syk tyrosine kinase to these receptor clusters.³⁷ Together with other reports,¹⁴ these data support the conclusion that dimerizing agents *can* activate the FcεRI, provided that crosslinking induces appropriate orientation or conformational changes in pairs of receptors.

Of note, the large signaling patches induced by multivalent antigen are often bordered by coated pits poised to internalize receptors (Figure 1B, arrow). This observation is highly reproducible, despite the fact that depletion of clathrin fails to inhibit FcεRI endocytosis after activation (ref³⁸ and our unpublished results). We speculate that, like the BCR,³⁹ compensatory non-clathrin mediated internalization pathways ensure that highly crosslinked FcεRI are removed from the mast cell surface.

GPCRs Bound to Monovalent Ligands also Form Signaling Patches

The N-formyl peptide receptor (FPR) is naturally co-expressed with the IgE receptor on human basophils. In a study of RBL-2H3 transfectants stably expressing the FPR, this GPCR was observed to form large clusters in response to addition of monovalent ligand.⁴⁰ Ligand-bound FPR cluster rapidly and recruit the heterotrimeric G-protein, Gi. FPR are slowly endocytosed and, by 5 min, most clusters remaining on the surface contain arrestin and very little Gi. We also found that, when ligands for **both** FPR and FcεRI were added simultaneously, there was a marked increase in colocalization of the two receptor clusters (Fig. 1E). This study suggested that crosstalk between the tyrosine kinase pathway of the FcεRI and the G-protein-coupled pathway of the FPR occurs locally. Barisas and colleagues have proposed that crosstalk between FcεRI and the inhibitory receptor, MAFA, may also occur in rafts or specialized domains.⁴¹ Together with evidence for clustering of growth factor receptors,^{42,43} These data also support the notion that receptor clustering is not solely a property of physical crosslinking by multivalent ligand (as is the case for FcεRI) but a more generalized architecture for receptors during active signaling.

Signaling Patches as Special Features of the Protein Island Network

Experiments comparing the distributions of *all proteins* in T cell and RBL membranes shed some light on the issue of colocalizing receptors.²⁷ When bulk membrane proteins were labeled for electron microscopy with probes targeted at SH-groups, the gold label concentrated in dark regions of membrane that also label for cholesterol. Furthermore, non-raft and raft markers were constructed by expressing tagged versions of N-terminus of Lck with and without mutation of the palmitoylation sites. Statistical analysis using the Ripley's

K function confirmed that the two markers were strongly segregated. These results led us to propose a new model for membrane organization, where proteins organize into complex, cholesterol-rich “islands” in a largely lipid sea. This hypothesis was recently supported by the sophisticated PALM technique (photoactivation localization microscopy).²⁸ We speculate that signaling patches represent specialized domains within islands that initiate, amplify and control signal propagation in a spatially restricted manner.

Single Particle Tracking Allows Direct Observation of Diffusing FcεRI

We have recently developed a method to directly observe the diffusive behavior of individual FcεRI, before and after crosslinking with ligands of different valency. As described in our recent publications,^{35,36} monovalent quantum dot (QD)-labeled IgE can be reliably prepared and used to “prime” FcεRI at sparse densities that allow for identification and tracking of individual QD-IgE-receptor complexes diffusing on the surface of live cells. The use of QDs provides several advantages. Their high brightness and photostability allows for long-term single molecule imaging. QDs have broad excitation, yet narrow emission, spectra allowing for simultaneous excitation and detection of spectrally distinct QDs using a single excitation wavelength and filter-based detection. The use of two- or four-color emission beam splitters and sensitive emCCD cameras permits fast and well-resolved collection of fluorescence from 2–4 spectrally distinct probes simultaneously at the single QD level.

Using single particle tracking, we have characterized the diffusive behavior of FcεRI (Figure 2A), which ranges from highly mobile to confined to immobile. Temperature plays a significant role, with ~ 2 fold faster diffusion and larger corral sizes measured at physiological temperature (35–37°C) as compared to room temperature.³⁵ Even in the resting state, a small fraction of receptors are found to be at least transiently immobile (classified by a diffusion coefficient $< 0.001\mu\text{m}^2/\text{s}$). Individual receptors can switch rapidly and apparently randomly between these diffusion states (see movies in ref³⁵).

The ability to distinguish two or more QD colors was a critical factor in determining whether resting FcεRI, observed by EM to be distributed in small clusters, interact with each other sufficiently strongly to drive the clustering. The best evidence for this possibility would be the detection of “correlated motion” over a significant period of time. As shown in Figure 2C–D, we often observe QD-labeled IgE receptors in close proximity. Figure 2C illustrates a case of two receptors which remain close ($< 500\text{ nm}$) for several seconds. However, the plot at the right shows that their movements remain uncorrelated. In Figure 2D, two receptors move close to each other for a short time then separate, moving over 2 microns apart before reversing directions and crossing paths again. Analysis of $> 1,000$ close-approach events imaged at 100 frames/sec revealed that correlated motion was not occurring, indicating that the resting receptors do not form a stable complex.³⁵ Thus, the most obvious interpretation is that resting FcεRI can briefly share residency in the same microdomain, but that their associations (if any) during this residency period are very weak. This is consistent with time-resolved phosphorescence polarization studies, which concluded that the rotational mobility of resting receptors is neither hindered by direct association with the cytoskeleton or by aggregation.¹⁰

Modeling the Ins and Outs of Resting Receptor Clusters

We have used stochastic modeling approaches to test the possibility that transient residency of resting receptors in islands or rafts provides a plausible explanation for their non-random distribution. For these simulations, the 2-D membrane is represented by a Cartesian plane with a periodic boundary such that receptors that leave the plane re-enter on the opposite side of the membrane. Species in the simulation are considered as individual particles or

agents that move at each time step under a Constrained Brownian Motion algorithm.⁴⁴ The membrane can be further subdivided into domains that are lipid-rich (fast diffusion for proteins) and protein-rich (2-fold slower diffusion for proteins in the simulation) (Figure 2E). Although we first applied this technique to the EGFR, the approach is applicable to virtually any resting membrane receptor (including FcεRI) provided diffusion rates are experimentally defined. Even if membrane proteins begin the simulation at random locations, a pattern of clustering will form that closely matches that observed by immunoelectron microscopy and similarly passes the Hopkins test (Figure 2F). We conclude that, even when receptors are in constant motion, short duration trapping in protein-rich microdomains (islands) can result in clustering.

Consistent with this hypothesis is prior evidence that FcεRI diffusion is profoundly influenced by protein crowding. Thomas et al³⁰ found that FcεRI slowed significantly within densely populated poles that developed on RBL cells exposed to electric fields. In that study, significant effects were revealed only on membranes of osmotically shocked RBL cells, which released constraints of the cortical cytoskeleton. Other experiments during the early 1990s demonstrated that crowding slows diffusion of membrane receptors in artificial bilayers.^{45,46} Of course, an intact cytoskeleton also exerts a strong influence on receptor diffusion, by serving as physical barriers or corrals³⁵ and by anchoring protein islands.²⁷ The cytoskeleton will be further discussed in sections below.

Immobilization of Crosslinked FcεRI is Dependent on Dose and Antigen Valency

Tracking of QD-IgE bound receptors permitted us, for the first time, to observe the transition from resting to crosslinked receptors in real time (Figure 3A). As predicted, based upon prior reports of FcεRI immobilization after crosslinking,^{4,12,47} we observed that stimulation with modest to high doses of highly polyvalent antigen (DNP₂₄-BSA, 0.1–10 μg/ml) resulted in rapid immobilization (Figure 3A). Our real-time assay was directly able to determine the kinetics of this change in mobility, found to occur in less than 20 s. Somewhat unexpectedly, we found that low doses of the same highly multivalent antigen failed to induce immobilization despite robust stimulation of degranulation.³⁶ We similarly found that even high doses of low valency antigens (DNP₂-BSA, DNP₄-BSA), also shown to induce degranulation, did not cause receptor immobilization (Figure 3B).

These results firmly lead to the conclusion that immobilization is not a requisite event for *signal initiation* from the crosslinked FcεRI. However, it is intriguing to consider this in the broader context of previous work using structurally defined ligands and dimerizing antibodies for FcεRI stimulation (reviewed in ref 14). There are strong correlations between *signaling potency* and the predicted oligomeric state of crosslinked receptors. Dimerizing reagents, including both divalent ligands and antibodies directed at either the FcεRI α subunit or at IgE, exhibit a wide range of stimulatory capacity. It is possible for such reagents to induce immobilization in the absence of signaling, at least as measured by degranulation and Ca²⁺ mobilization.⁴⁸ Bivalent ligands with flexible PEG-based spacers fail to stimulate measurable secretion⁴⁹ and can even be inhibitory.⁵⁰ In general, higher oligomers induced by higher valency antigens – or further crosslinking of antibody-bound complexes – generate better signaling from the RBL-2H3 cell line over a broad dose response range. A number of factors have been implicated, including overriding constraints imposed by cyclic dimers as well as the improved geometry, spacing and orientation of receptors in large aggregates (see discussion in ref 14). Lateral forces may also be a factor, based upon observations that liposomes or lipid bilayers bearing haptens for IgE can recruit large numbers of receptors to the adhesive surface and can induce weak but measurable secretory responses.^{51–53} IgE-FcεRI complexes engaged by lipid-conjugated monovalent

happen form a “synapse” and induce degranulation while remaining highly mobile, further demonstrating that immobilization is not required for signal initiation.⁵³

We note that maximal secretory responses of bone marrow derived mast cells (BMDC) and human basophils occur over a much narrower range even for the highly polyvalent antigens,^{36,54} often abruptly dropping off at modest concentrations of crosslinking reagents. This phenomenon has been referred to as “high dose inhibition” and may be attributed to active negative regulatory mechanisms that dominate in FcεRI-bearing primary cells. In support of this, we found that receptor immobilization can trigger internalization even in the absence of signaling.³⁶

The Influence of the Cortical Cytoskeleton

The actin cytoskeleton has long been proposed to form “corrals” or “picket fences” capable of restricting movements of membrane proteins.^{56–58} By coupling QD-IgE single particle tracking with TIRF (total internal reflection microscopy), we were able to directly test this widely-held theory.³⁵ To perform this series of experiments, RBL cells were selected that stably express GFP-actin. The movements of resting QD-labeled IgE receptors were then tracked relative to actin filaments at the lightly adherent surface of live cells settled on coverslips. Images were captured at a rate of 35–100 frames/second. As illustrated in Figure 3C, QD-labeled receptors were shown to be markedly restricted by the network of actin cables juxtaposed to the inner membrane. Moreover, because the actin network is dynamic, the shapes of the corrals were shown to be constantly changing and therefore frequently permit QD-labeled receptors to “slip” between openings to previously inaccessible compartments.

The GFP-actin cables, seen by TIRF, span distances of several microns. We have used high resolution microscopy techniques to capture fine details of cortical cytoskeletal elements that are too fine to resolve in the fluorescence microscope, even in TIRF mode that helps to eliminate out-of-focus light.^{59,60} The image in Figure 3D shows the topographic detail of the cytoplasmic face of a hydrated membrane sheet prepared from an RBL cell. It was acquired on the AFM (Atomic Force Microscope) of our collaborator, Alan Burns, at Sandia National Laboratory. The image is pseudo-colored to indicate heights ranging from 5–6 nm (dark red, the width of a lipid bilayer) to 30 nm (hot yellow) above the substrate. Raised domains dot the landscape and are connected by many thin filaments. This image, and others obtained on the transmission electron microscope (see cables in the images in Figure 1), led us to conclude that the cortical cytoskeleton links protein islands in the RBL membrane. We found that labels for actin and myosin do not uniformly label the fine meshwork.⁵⁹ Instead actin and myosin are usually concentrated at junctions in the network. This leads us to speculate that actin bundles are only a minor fraction of the network, providing an explanation for the fact that latrunculin treatment only modestly enhances the mobility of molecules in single particle tracking experiments.^{61,35} Lillemeier and colleagues²⁷ found that protein islands are smaller but persistent in T cell membranes when their cytoskeletal tethers are disrupted by latrunculin treatment. Dense cytoskeletal networks or direct associations with crosslinked FcεRI may actually limit the signaling process, as suggested by the work of Seagrave and Oliver³³ and Holowka and Baird.⁶² Seagrave and Oliver⁶³ noted that cytochalasin treatment reduced the size of FcεRI aggregates observed by SEM, leading to the hypothesis that very large aggregates signal poorly.

Intracellular Protein-Protein Interactions Provide an Additional Mechanism to Stabilize Signaling Patches: the Case of LAT

Like other immunoreceptors, signal propagation following FcεRI crosslinking involves the recruitment of a large number of proteins that contain binding motifs, such as SH2 (src homology 2), SH3 (src homology 3), PH domains, PTB domains and others.^{3,64} Large macromolecular complexes can form based on these interactions, with the potential to induce aggregation and stabilize clusters of receptors and other signaling proteins. Goldstein and colleagues have used mathematical modeling to validate intracellular cross-bridging as a mechanism for growth and stabilization of large clusters of the scaffolding protein, Linker for Activation of T cells (LAT).⁶⁵ The model is based upon the ability of Grb2 to bind via its SH2 domain to phosphorylated LAT and to two molecules of SOS through its two SH3 domains.^{66,67} Thus multivalent, cooperative protein-protein interactions that propagate at the cytoplasm-membrane interface may explain, in large part, the observation that LAT clusters markedly increase in size following FcεRI crosslinking⁵⁹ or TCR activation.^{28,67} It seems likely that this paradigm will be broadly applicable to other transmembrane proteins that participate in complex signaling cascades.

What about Lipids?

The local lipid environment of immunoreceptors remains enigmatic. In 2002, Jacobson and Anderson proposed that membrane proteins might be surrounded by a lipid shell.⁶⁸ Proof for this attractive concept has eluded investigators to date, mostly because of technical limitations. However, evidence for strong lipid association with FcεRI dates back to the work of Rivnay, Metzger and colleagues.^{69,70} The addition of lipids to detergent micelles delayed the slow dissociation of FcεRI subunits, with the best protection provided by dipalmitoylglycerol and cholesterol.⁷¹

If a lipid shell envelopes FcεRI, cholesterol is perhaps our best candidate. However, results from multiple laboratories remain complex and, in our opinion, controversial. For example, RBL cells depleted of cholesterol after mBCD treatment show profound defects in membrane topography, including widespread “flat” clathrin arrays and reduced overall height of all membrane domains.⁶⁰ These broad effects make it difficult to interpret differing reports that cholesterol depletion either inhibits the entire FcεRI tyrosine kinase cascade⁷² or has little effect on FcεRI-induced phosphorylation but differential effects on calcium mobilization and degranulation.^{73,74}

We have focused on alternative approaches to evaluate the lipid environment of FcεRI in resting and activated states. We previously made use of the capabilities of X-ray spectral electron microscopy,⁷⁵ where specific elements in the sample emit characteristic X-rays when excited by the electron beam and the intensity of the signal relates to its concentration. Data can be acquired in scanning mode on STEM instruments, reporting pixel-by-pixel values for specific elements at nanometer resolution; operating in TEM mode, one also can acquire a more traditional image of the sample that is based on contrast. We focused on the distribution of osmium, a contrast agent commonly used in electron microscopy due to its ability to react with double bonds in lipids. As shown in Fig. 4A, this method revealed that membranes concentrate osmium in patches on the membrane; and this observation strongly suggested that lipids with double bonds (a category that includes cholesterol) were unequally distributed.

Our next approach was to isolate plasma membrane-derived vesicles for lipidomics analysis in collaboration with Robert Murphy (Univ. of Colorado), with a primary goal of avoiding detergent expected to disrupt native structure. Our strategy was to crosslink IgE receptors or

GPI-anchored Thy-1 on the surface of RBL cells with specific antibodies, forming large patches enriched in either activated receptors or aggregated Thy-1.⁷⁶ Cells were rapidly chilled and mechanically disrupted to vesiculate the plasma membrane. After a series of steps to reduce contamination from unbroken cells, etc, we then used immunomagnetic bead isolation to isolate right-side-out vesicles containing IgE receptors or Thy-1. Enrichment was confirmed by 2-D gel electrophoresis (to evaluate the protein content) and then samples were prepared and sent to Denver. This process was repeated over several years for an in depth analysis of the levels of fatty acid saturation, cholesterol levels and lipid composition. This study generated several significant findings: 1) Both vesicle preparations contained a complex set of plasma membrane phospholipids, as analyzed by mass spec analysis; 2) Lipid content in vesicles immuno-isolated with anti-IgE was 50% cholesterol, compared to less than 25% in Thy-1 vesicles (Fig. 4B); 3) Less than 50% of the fatty acids in either domain were saturated, inconsistent with the concept of liquid ordered domains; and 4) IgE receptor-containing vesicles contained 2–3 times more sphingomyelin and plasmalogens than the Thy-1 domains. The plasmalogen finding is particularly intriguing, since the vinyl ether linkage at the sn-1 position introduces a double bond that is very near the lipid head group. Plasmalogens were also found to be enriched in lipid raft fractions containing the EGFR.⁷⁷ Although plasmalogens are widely distributed in nature, roles for these lipids remain poorly defined. Remarkably, new mouse models with ether lipid deficiencies have severe defects, including arrest of spermatogenesis, cataracts and deficiencies in CNS myelination. These problems have been linked to impaired intracellular cholesterol distribution, plasma membrane function and ER/Golgi structural changes (reviewed in ref 78). On an interesting note, mast cells from cholesterol-deficient SLOS mice exhibit hyperdegranulation and constitutive cytokine production, which may be linked to down regulation of Lyn acting in its negative regulatory role.⁷⁹

Recently we employed new strategies to allow us to track cholesterol in live cells. Working with Jeri Timlin at Sandia National Laboratories, we have tested several fluorescent cholesterol derivatives in RBL-2H3 cells. Our best success is with cholesterol-18 FITC that has a long linker for the chromophore (Figure 4C). This probe is easily tracked when imaging in TIRF mode and forms patches that markedly travel and colocalize with FcεRI recruited to lipid bilayers presenting monovalent, mobile ligands.⁵³ These patches are remarkably similar to the microclusters of TCR and BCR that travel to the well described synapses of T cells⁸⁰ and B cells.⁸¹ This was the first evidence that microclusters of immunoreceptors are enriched in cholesterol as they move to the synapse.

It remains to be determined which of cholesterol's biochemical and biophysical properties predominate in the regulation of membrane architecture: its ability to influence membrane rigidity and fluidity; its affinity for sphingolipids and disaturated phosphatidylserine;⁸² its ability to bind directly to specific proteins;^{83,84} or its importance for membrane curvature.⁸⁵ For the FcεRI, we are struck by the enigma of its association with mobile, but not immobile, receptors at the immune synapse.⁵³ If cholesterol comprises part of the lipid shell around FcεRI, it must be sufficiently weak that dissociation occurs if receptors become trapped by binding to an immobile ligand. Since receptors trapped in this way cause massive degranulation, it also appears that cholesterol is not an absolute requirement for signal transduction to commence.

Concluding Remarks and Future Directions

As the entry point for signaling input, the plasma membrane continues to be the focus of intense study. Its constituents occupy a surprisingly complex 2-D environment, where interactions are dependent on encounters in confined and constantly rearranging spaces. Perhaps the greatest next challenge is to capture the subsecond temporal details of signal

transducers recruited to FcεRI oligomers stimulated with defined ligands, as well as to downstream signaling scaffolds such as LAT. This will be an important goal, since population readouts such as phosphorylation patterns of FcεRI β, Syk and LAT fail to correlate well with downstream responses such as degranulation.⁸⁶

We anticipate the development of such measurements in the near future, since innovation has been a hallmark of the mast cell imaging community, often leading the way for the entire field of receptor biology. Examples include the development of GFP/SH2 and GFP-PH domain fusion proteins as reporters of protein translocation to the plasma membrane probes in response to FcεRI activation.⁸⁷ Fluorescence correlation spectroscopy (FCS) has been creatively applied by the collaborative team of Webb, Baird and Holowka⁸⁸ to measure association between FcεRI and Lyn tyrosine kinase on live cells following antigen stimulation. This important subject deserves revisiting, since the authors' choice of room temperature measurements (to slow internalization and membrane ruffling) likely also delayed the apparent time course of Lyn recruitment (5–6 min after antigen addition). Our group has developed multi-color quantum dot probes to directly observe the formation of FcεRI aggregates, to track the correlated motion of small aggregates and to observe the abrupt immobilization of larger aggregates.^{35,36} FCS and SPT represent powerful technologies for measuring the dynamics of protein-protein interactions. In addition, emerging super-resolution and correlation imaging technologies hold much promise for the quantitative measurement of protein-protein interactions in living cells (reviewed in ref 89). Such advances in imaging techniques will allow us to take the next step - beyond the plasma membrane - to look at the cytoplasmic protein dynamics and interactions that propagate the message initiated by FcεRI aggregation.

Acknowledgments

This work was supported by NIH R01AI051575 (BSW), NIH RO1GM49814 (JMO), the Human Frontiers Science Program (DSL), NIH SPORE M01RR000997 and NIH P50GM085273 (that supports the New Mexico Spatiotemporal Modeling Center). We acknowledge important institutional resources, particularly the UNM Cancer Center Fluorescence Microscopy Facility and the Electron Microscopy Facility. We acknowledge present and former members of the Cell Pathology laboratory for their important contributions, particularly Mary Ann Raymond-Stintz, Angela Welford, Nicholas Andrews, Janet Pfeiffer, Zurab Surviladze, Genie Hsieh, Mei Xue and Amanda Carroll-Portillo whose work is included in this summary. We also thank our collaborators at UNM (Keith Lidke, Stanly Steinberg, Jeremy Edwards), Sandia National Laboratory (Alan Burns, Jerilyn Timlin, Paul Kotula), Los Alamos National Laboratory (Byron Goldstein, Bill Hlavacek), University of Notre Dame (Basar Bilgicer) and University of Colorado (Robert Murphy) for scientific contributions and valuable discussion.

References

1. Wasserman SI. Basic mechanisms in asthma. *Ann Allergy*. 1988; 60:477–82. [PubMed: 3163472]
2. Gilmartin L, Schuyler M, Pickett G, et al. A comparison of inflammatory mediators released by basophils of asthmatic and control subjects in response to high affinity IgE receptor aggregation. *Inter Arch Allergy & Immun*. 2007; 145:182–192.
3. Gifillan A, Rivera J. The tyrosine kinase network regulating mast cell activation. *Immunological Reviews*. 2009; 228:149–169. [PubMed: 19290926]
4. Schlessinger J, Webb WW, Elson EL, et al. Lateral motion and valence of Fc receptors on rat peritoneal mast cells. *Nature*. 1976; 264:550–552. [PubMed: 1004593]
5. McCloskey MA, Liu ZY, Poo MM. Lateral electromigration and diffusion of Fc epsilon receptors on rat basophilic leukemia cells: effects of IgE binding. *J Cell Biol*. 1984; 99:778–787. [PubMed: 6236227]
6. Zhang W, Samelson LE. The role of membrane-associated adaptors in T cell receptor signalling. *Semin Immunol*. 2000; 12:35–41. [PubMed: 10723796]

7. Pecht I, Ortega E, Jovin TM. Rotational dynamics of the Fc epsilon receptor on mast cells monitored by specific monoclonal antibodies and IgE. *Biochemistry*. 1991; 30:3450–3458. [PubMed: 1849426]
8. Myers JN, Holowka D, Baird B. Rotational motion of monomeric and dimeric immunoglobulin E-receptor complexes. *Biochemistry*. 1992; 31:567–75. [PubMed: 1310043]
9. Ryan TA, Myers J, Holowka D, et al. Molecular crowding on the cell surface. *Science*. 1988; 239:61–4. [PubMed: 2962287] Thomas JL, Holowka D, Baird B, et al. Large-scale coaggregation of fluorescent lipid probes with cell-surface proteins. *J Cell Biol*. 1994; 125:795–802. [PubMed: 8188747]
10. Zidovetzki R, Bartholdi M, Arndt-Jovin D, et al. Rotational dynamics of the Fc receptor for immunoglobulin E on histamine-releasing rat basophilic leukemia cells. *Biochemistry*. 1986; 25:4397–4401. [PubMed: 2428396]
11. Feder TJ, Brust-Mascher I, Slatery JP, et al. Constrained diffusion or immobile fraction on cell surfaces: a new interpretation. *Biophys J*. 1996; 70:2767–73. [PubMed: 8744314]
12. Menon AK, Holowka D, Webb WW, Baird B, et al. Crosslinking of receptor-bound IgE to aggregates large than dimers leads to rapid immobilization. *J Cell Biol*. 1986a; 102:541–550. [PubMed: 2935543]
14. Holowka D, Swaipayan S, Torigoe C, et al. Insights into immunoglobulin E receptor signaling from structurally defined ligands. *Immunological Reviews*. 2007; 217:269–279. [PubMed: 17498065]
16. Brown DA, Rose JK. Sorting of GPI-anchored proteins to glycolipid-enriched membrane subdomains during transport to the apical cell surface. *Cell*. 1992; 68:533–44. [PubMed: 1531449]
17. Simons K, Ikonen E. Functional rafts in cell membranes. *Nature*. 1997; 387:569–572. [PubMed: 9177342]
18. Ahmed SN, Brown DA, London E. On the origin of sphingolipid/cholesterol-rich detergent-insoluble cell membranes: physiological concentrations of cholesterol and sphingolipid induce formation of a detergent-insoluble, liquid-ordered lipid phase in model membranes. *Biochemistry*. 1997; 36:10944–53. [PubMed: 9283086]
19. Field KA, Holowka D, Baird B. FcεRI-mediated recruitment of p53/56(lyn) to detergent-resistant membrane domains accompanies cellular signaling field. *Proc Natl Acad Sci USA*. 1995; 92:9201–9205. [PubMed: 7568101]
20. Field KA, Holowka D, Baird B. Compartmentalized activation of the high affinity immunoglobulin E receptor within membrane domains. *J Biol Chem*. 1997; 272:4276–4280. [PubMed: 9020144]
21. Field KA, Holowka D, Baird B. Structural aspects of the association of FcεRI with detergent-resistant membranes. *J Biol Chem*. 1999; 274:1753–1758. [PubMed: 9880557]
22. Draberova L, Draber P. Thy-1 glycoprotein and src-like protein-tyrosine kinase p53/p56(lyn) are associated in large detergent-resistant complexes in rat basophilic leukemia-cells. *Proc Natl Acad Sci USA*. 1993; 90:3611–3615. [PubMed: 7682713]
23. Vereb G. Dynamic, yet structured: The cell membrane three decades after the Singer-Nicolson model. *Proc Natl Acad Sci USA*. 2003; 100:8053–8. [PubMed: 12832616]
24. Lagerholm BC. Detecting microdomains in intact cell membranes. *Annu Rev Phys Chem*. 2005; 56:309–36. [PubMed: 15796703]
25. Hancock JF. Lipid rafts: contentious only from simplistic standpoints. *Nat Rev Mol Cell Biol*. 2006; 7:456–62. [PubMed: 16625153]
26. Jacobson K, Mouritsen OG, Anderson RG. Lipid rafts: at a crossroad between cell biology and physics. *Nat Cell Biol*. 9:7–14. [PubMed: 17199125]
27. Lillemeier BF, Pfeiffer JR, Surviladze Z, et al. Plasma membrane-associated proteins are clustered into “islands” attached to the cytoskeleton. *Proc Natl Acad Sci USA*. 2006; 103:18992–18997. [PubMed: 17146050]
28. Lillemeier BF, Mörtelmaier MA, Forstner MB, et al. TCR and Lat are expressed on separate protein islands on T cell membranes and concatenate during activation. *Nature Immunol*. 2010; 11:90–96. [PubMed: 20010844]
29. Yechiel E, Edidin M. Micrometer-scale domains in fibroblast plasma membranes. *J Cell Biol*. 1987; 105:755–760. [PubMed: 3624308]

30. Thomas JL, Feder TJ, Webb WW. Effects of protein concentration on IgE receptor mobility in rat basophilic leukemia cell plasma membranes. *Biophys J*. 1992; 61:1402–12. [PubMed: 1534697]
31. Douglass AD, Vale RD. Single-molecule microscopy reveals plasma membrane microdomains created by protein-protein networks that exclude or trap signaling molecules in T cells. *Cell*. 2005; 121:937–950. [PubMed: 15960980]
32. Stump RF, Pfeiffer JR, Seagrave J, et al. Mapping gold-labeled IgE receptors on mast cells by scanning electron microscopy: receptor distributions revealed by silver enhancement, backscattered electron imaging, and digital image analysis. *J Histochem Cytochem*. 1988; 36:493–502. [PubMed: 2965720]
33. Surviladze Z, Dráberová L, Kovárová L, et al. Differential sensitivity to acute cholesterol lowering of activation mediated via the high-affinity IgE receptor and Thy-1 glycoprotein. *Eur J Immunol*. 2001; 31:1–10. [PubMed: 11169432]
34. Seagrave J, Pfeiffer JR, Wofsy C, et al. Relationship of IgE receptor topography to secretion in RBL-2H3 mast cells. *J Cell Physiol*. 1991; 148:139–151. [PubMed: 1830592]
34. Wilson BS, Pfeiffer JR, Oliver JM. Observing FcεRI signaling from the inside of the mast cell membrane. *J Cell Biol*. 2000; 149:1131–1142. [PubMed: 10831616]
35. Andrews NL, Lidke KA, Pfeiffer JR, et al. Actin restricts FcεRI diffusion and facilitates antigen-induced receptor immobilization. *Nat Cell Biol*. 2008; 10:955–963. [PubMed: 18641640]
36. Andrews NL, Pfeiffer JR, Martinez AM, et al. Small, mobile FcεRI aggregates are signaling competent. *Immunity*. 2009; 31:469–479. [PubMed: 19747859]
37. Lara M, Ortega E, Pecht I, et al. Aggregating Lyn-sequestering FcεRI dimers restores signaling overcoming the signaling defect of Lyn-sequestering, signal-curtailling FcεRI dimers: aggregating the dimers allows phosphorylated FcεRI to dissociate from Lyn and form signaling complexes with Syk in specialized membrane domains. *J Immunol*. 2001; 167:4329–4337. [PubMed: 11591756]
38. Fattakhova G, Masilamani M, Borrego F, Metcalfe AMDD, Coligan JE, et al. The high-affinity immunoglobulin-E receptor (FcεRI) is endocytosed by an AP-2/clathrin-independent, dynamin-dependent mechanism. *Traffic*. 2006; 7:673–685. [PubMed: 16637889]
39. Stoddart A, Jackson AP, Brodsky FM. Plasticity of B cell receptor internalization upon conditional depletion of clathrin. *Mol Biol Cell*. 2005; 16:2339–48. [PubMed: 15716350]
40. Xue M, Hsieh G, Raymond-Stintz M, et al. FPR and FcεRI occupy common domains for signaling and internalization. *Mol Biol Cell*. 2007; 18:1410–1420. [PubMed: 17267694]
41. Barisas BG, Smith SM, Liu J, et al. Compartmentalization of the Type I Fc ε receptor and MAFA on mast cell membranes. *Biophys Chem*. 2007; 126:209–17. [PubMed: 16797115]
42. Nagy P, Jenei A, Kirsch AK, et al. Activation-dependent clustering of the erbB2 receptor tyrosine kinase detected by scanning near-field optical microscopy. *J Cell Sci*. 1999; 112:1733–41. [PubMed: 10318765]
43. Yang S, Raymond-Stintz MA, Ying W, et al. Mapping ErbB receptors on breast cancer cell membranes during signal transduction. *J Cell Science*. 2007; 120:2763–2773. [PubMed: 17652160]
44. Hsieh W, Shu W, Yang S, et al. Stochastic simulations of ErbB homo and hetero-dimerization: potential impacts of receptor conformational state and spatial segregation. *IET Systems Biology*. 2008; 2:256–272. [PubMed: 19045821]
45. Tank DW, Wu E-S, Webb WW. Enhanced molecular diffusibility in muscle membrane blebs: release of lateral constraints. *J Cell Biol*. 1982; 92:207–212. [PubMed: 7199052]
46. Peters R, Cherry RJ. Lateral and rotational diffusion of bacteriorhodopsin in lipid bilayers: experimental test of the Saffman-Delbruck equations. *Proc Natl Acad Sci USA*. 1982; 79:4317–4321. [PubMed: 6956861]
47. Menon AK, Holowka D, Webb WW, Baird B, et al. Clustering, mobility and triggering activity of small oligomers of immunoglobulin E on rat basophilic leukemia cells. *J Cell Biol*. 1986b; 102:534–540. [PubMed: 2418032]
48. Posner RF, Subramanian K, Goldstein B, et al. Simultaneous cross-linking by two nontriggering bivalent ligands causes synergistic signaling of IgE FcεRI complexes. *J Immunology*. 1995; 155:3601–3609. [PubMed: 7561059]

49. Posner RG, Geng D, Haymore S, et al. Trivalent antigens for degranulation of mast cells. *Org Lett.* 2007; 9:3551–4. [PubMed: 17691795]
50. Baird EJ, Holowka D, Coates G, et al. Highly effective poly(ethylene glycol) architectures for specific inhibition of immune receptor activation. *Biochemistry.* 2003; 42:12739–48. [PubMed: 14596588]
51. McConnell HM, Watts TH, Weis RM, et al. Supported planar membranes in studies of cell-cell recognition in the immune system. *Biochim Biophys Acta.* 1986; 864:95–106. [PubMed: 2941079]
52. McCloskey MA, Poo MM. Contact-induced redistribution of specific membrane components: local accumulation and development of adhesion. *J Cell Biol.* 1986; 102:2185–2196. [PubMed: 2423534]
53. Carroll-Portillo A, Spendier K, Pfeiffer J, et al. FcεRI membrane dynamics upon binding mobile or immobile ligands on surfaces: formation of a mast cell synapse. *J Immunology.* 2010; 184:1328–1338. [PubMed: 20042583]
54. Kepley CL, Wilson BS, Oliver JM. Roles for the protein tyrosine kinases Lyn, Syk and Zap-70 in FcεRI-mediated human basophil degranulation. *J of Clinical Allergy and Immunology.* 1998; 102:304–315.
56. Sheetz MP. Membrane skeletal dynamics: role in modulation of red cell deformability, mobility of transmembrane proteins, and shape. *Semin Hematol.* 1983; 20:175–188. [PubMed: 6353589]
57. Saxton MJ. Single particle tracking: effects of corrals. *Biophysical J.* 1995; 69:389–396.
58. Kusumi A, Ike H, Nakada C, et al. Single-molecule tracking of membrane molecules: plasma membrane compartmentalization and dynamic assembly of raft-philic signaling molecules. *Semin Immunol.* 2005; 1:3–21. [PubMed: 15582485]
59. Wilson BS, Pfeiffer JR, Surviladze Z, et al. High resolution mapping reveals distinct FcεRI and LAT domains in activated mast cells. *J Cell Biol.* 2001; 154:645–658. [PubMed: 11489921]
60. Frankel DJ, Pfeiffer J, Oliver JM, et al. Revealing the topography of cellular membrane domains by combined atomic force microscopy/fluorescence imaging. *Biophysical J.* 2006; 90:2404–2413.
61. Fujiwara T, Ritchie K, Murakoshi H, et al. Phospholipids undergo hop diffusion in compartmentalized cell membrane. *J Cell Biol.* 2002; 157:1071–81. [PubMed: 12058021]
62. Pierini L, Harris NT, Holowka D, et al. Evidence supporting a role for microfilaments in regulating the coupling between poorly dissociable IgE-FcεRI aggregates downstream signaling pathways. *Biochemistry.* 1997; 36(7):447–56.
63. Seagrave J, Oliver JM. Antigen-dependent transition of IgE to a detergent-insoluble form is associated with reduced IgE receptor-dependent secretion from RBL-2H3 mast cells. *J Cell Physiol.* 1990; 144:128–36. [PubMed: 2142164]
64. Zhang J, Leiderman K, Pfeiffer JR, et al. Characterizing the topography of membrane receptors and signaling molecules from spatial patterns obtained using nanometer-scale electron-dense probes and electron microscopy. *Micron.* 2006; 37:14–34. [PubMed: 16081296]
65. Nag A, Monine MI, Faeder JR, et al. Aggregation of membrane proteins by cytosolic cross-linkers: theory and simulation of the LAT-Grb2-SOS1 system. *Biophys J.* 2009; 96:2604–23. [PubMed: 19348745]
66. Houtman JC, Yamaguchi H, Barda-Saad M, et al. Oligomerization of signaling complexes by the multipoint binding of GRB2 to both LAT and SOS1. *Nat Struct Mol Biol.* 2006; 13:798–805. [PubMed: 16906159]
67. Bunnell SC, Singer AL, Hong DI, et al. Persistence of cooperatively stabilized signaling clusters drives T-cell activation. *Mol Cell Biol.* 2006; 26:7155–66. [PubMed: 16980618]
68. Anderson RGW, Jacobson K. A role for lipid shells in targeting proteins to caveolae, rafts and other lipid domains. *Science.* 2002; 296:1821–1825. [PubMed: 12052946]
69. Rivnay G, Wank SA, Poy B, Metzger H, et al. Phospholipids stabilize the interaction between the a and b subunits of the solubilized receptor for immunoglobulin E. *Biochemistry.* 1982:6922–6927. [PubMed: 6218820]
70. Rivnay B, Fischer B. Phospholipid distribution in the microenvironment of the immunoglobulin E receptor from rat basophilic leukemia cell membrane. *Biochemistry.* 1986; 25:5686–5693. [PubMed: 2946319]

71. Kinet JP, Quarto R, Perez-Montfort R, et al. Noncovalently and covalently bound lipid on the receptor for immunoglobulin E. *Biochemistry*. 1985;7342–7348. [PubMed: 2935189]
72. Sheets ED, Holowka D, Baird B. Critical role for cholesterol in lyn-mediated tyrosine phosphorylation of FcεRI and their association with detergent-resistant membranes. *J Cell Bio*. 1999; 145:877–887. [PubMed: 10330413]
73. Surviladze Z, Harrison HA, Murphy RC, et al. FcεRI and Thy-1 domains have unique protein and lipid compositions. *J of Lipid Research*. 2007; 48:1325–1335. [PubMed: 17387221]
74. Yamashita T, Yamaguchi T, Murakami K, et al. Detergent resistant membrane domains are required for mast cell activation but dispensable for tyrosine phosphorylation upon aggregation of the high affinity receptor for IgE. *J Biochem*. 2001; 129:861–868. [PubMed: 11388899]
75. Wilson BS, Steinberg SL, Liederman K, et al. Distinct distribution and behavior of raft markers in native membranes. *Mol Biol Cell*. 1004; 15:2580–2592. [PubMed: 15034144]
76. Tamir I, Schweitzer-Stenner R, Pecht I. Immobilization of the type I receptor for IgE initiates signal transduction in mast cells. *Biochemistry*. 1996; 35:6872–83. [PubMed: 8639639]
77. Pike LJ, Han X, Gross RW. Epidermal growth factor receptors are localized to lipid rafts that contain a balance of inner and outer leaflet lipids: a shotgun lipidomics study. *J Biol Chem*. 2005; 280:26796–804. [PubMed: 15917253]
79. Kovarova M, Wassif CA, Odom S, et al. Cholesterol deficiency in a mouse model of Smith-Lemli-Opitz syndrome reveals increase mast cell responsiveness. *J Exp Med*. 2006; 203:1161–1171. [PubMed: 16618793]
80. Dustin ML. A dynamic view of the immunological synapse. *Semin Immunol*. 2005; 17:400–410. [PubMed: 16266811]
81. Tolar P, Hanna J, Krueger PD, et al. The constant region of the membrane immunoglobulin mediates B cell-receptor clustering and signaling in response to membrane antigens. *Immunity*. 2009; 30:44–55. [PubMed: 19135393]
83. Thiele C. Cholesterol binds to synaptophysin and is required for biogenesis of synaptic vesicles. *Nat Cell Biol*. 2000; 2:42–9. [PubMed: 10620806]
84. Epand RM. Cholesterol and the interaction of proteins with membrane domains. *Prog Lipid Res*. 2006; 45:279–94. [PubMed: 16574236]
85. Huttner WB, Zimmerberg J. Implications of lipid microdomains for membrane curvature, budding and fission. *Curr Opin Cell Biol*. 2001; 13:478–84. [PubMed: 11454455]
86. Paar JM, Harris NT, Holowka D, et al. Bivalent ligands with rigid double-stranded DNA spacers reveal structural constraints on signaling by FcεRI. *J Immunol*. 2002; 15:856–64. [PubMed: 12097389]
87. Stauffer TP, Meyer T. Compartmentalized IgE receptor-mediated signal transduction in living cells. *J Cell Biol*. 1997; 139:1447–1454. [PubMed: 9396750]
88. Larson DR, Gosse JA, Holowka DA, et al. Temporally resolved interactions between antigen-stimulated IgE receptors and Lyn kinase on living cells. *J Cell Biol*. 2005; 171:527–536. [PubMed: 16275755]
89. Lidke DS, Wilson BS. Caught in the act: quantifying protein behaviour in living cells. *Trends in Cell Biology*. 2009; 19:566–574. [PubMed: 19801189]

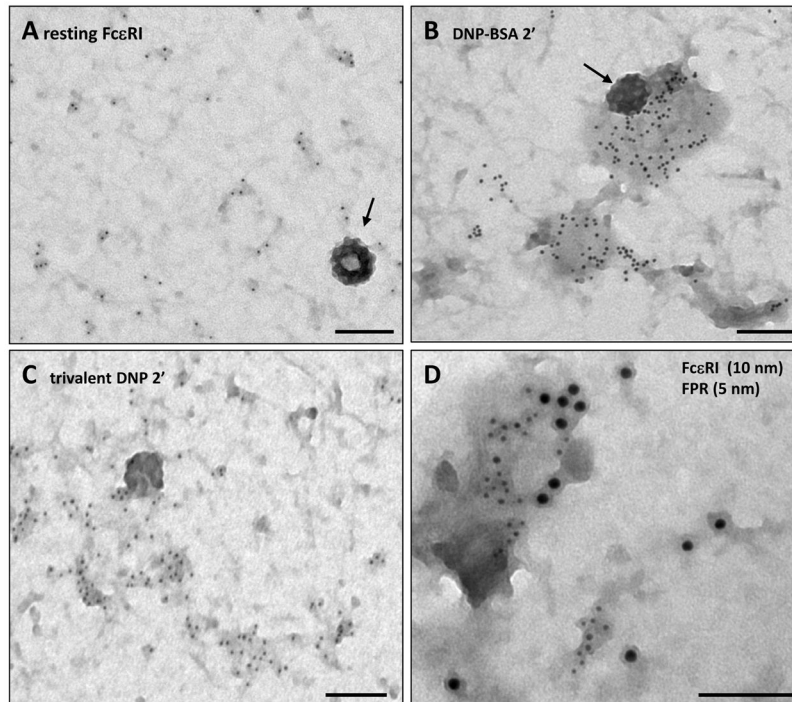


Figure 1. Electron microscopy reveals the spatial distribution of membrane receptors

A) RBL membrane sheets labeled with immunogold as in ref 34 to show that resting FcεRI are found as singlets and in small clusters. Arrow marks a clathrin-coated pit. (B) Two min after stimulation with 0.1 μg/ml DNP₂₄-BSA, larger clusters are seen to form. (C) Cells stimulated with a PEG-based flexible trivalent DNP ligand (10 nM) also demonstrate extensive FcεRI aggregation. (D) Simultaneous activation FcεRI (10 nm gold) and FPR (5 nm gold) leads to co-clustering of the receptors. Scale bars = 100 nm.

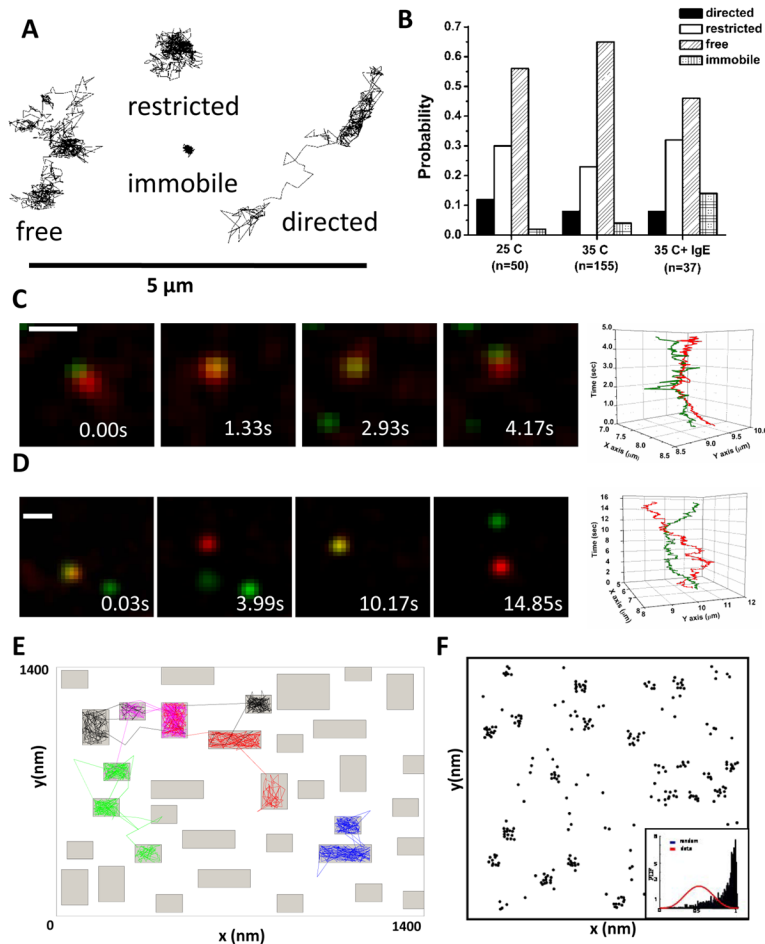


Figure 2. Characterizing Fc ϵ RI diffusion

(A) Example trajectories of individual Fc ϵ RI motion as determined by single quantum dot tracking. The expected four modes of motion are observed: free, restricted, directed and immobile (see Andrews et al., 2008). (B) Distribution of the modes of motion under different conditions. (C,D) Two-color imaging allows us to simultaneously track receptors labeled with QD655-IgE and QD585-IgE. Note that receptors often maintain close proximity but do not demonstrate correlated motion, indicating that the close proximity is due to co-confinement in a microdomain, not receptor interactions. (E) Example simulation from the Constrained Brownian Motion algorithm. Proteins in the simulation are considered as individual particles or agents that move at each time step (see ref 44). The membrane can be further subdivided into domains that are lipid-rich (fast diffusion for proteins, white space) and protein-rich (2-fold slower diffusion for proteins in the simulation, grey regions). Slower movement of receptors through the protein-rich domains leads to clustering of resting receptors (F) similar to that seen in electron microscopy images (Fig 1).

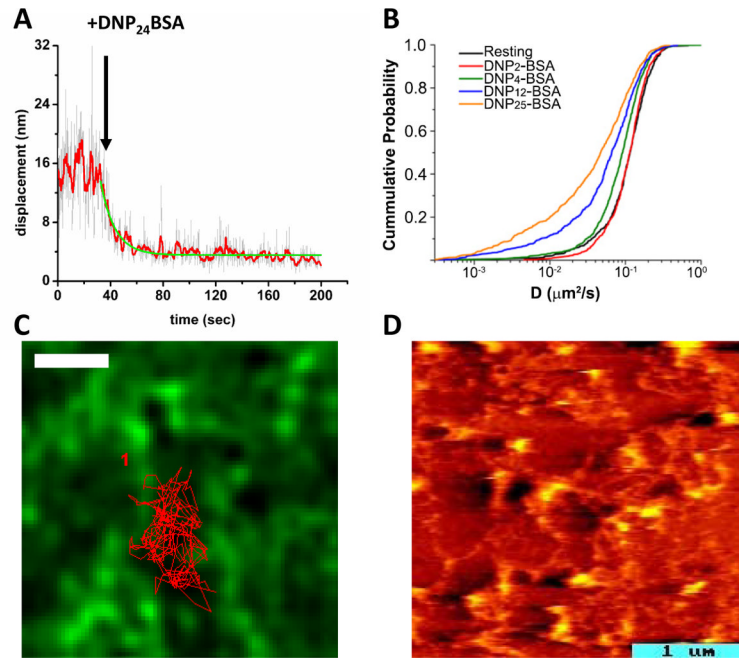


Figure 3.

(A) Plot of the average displacement of QD-IgE-FcεRI complexes between subsequent frames over the time course of a single movie. After addition of 1 μg/ml DNP₂₄-BSA, the displacement is seen to rapidly decrease, indicating a slow-down in receptor mobility (see ref 35). Red line is 10 frame averaging. Green line is exponential fit to the decay. (B) Cumulative Probability Analysis plot comparing the diffusion coefficients (D) of QD-IgE-FcεRI before and after crosslinking with antigens of different valency. Note that with DNP₂-BSA (red) receptor mobility did not change from resting (black) even though degranulation was seen under these conditions. Higher valencies did cause receptor slow-down, presumably due to the formation of larger aggregates (see ref 36). (C) Tracking of QD-IgE-FcεRI on cells expressing GFP-actin (green) shows that the receptor trajectory (red line) is confined by the actin cytoskeleton (green). Here, cells were treated with PMA that stabilized the actin filaments (see ref 35). Scale bar, 1 μm. (D) AFM image revealing the topography of the cytoplasmic face of an RBL membrane sheet. The image is pseudo-colored to indicate heights ranging from 5–6 nm (dark red, the width of a lipid bilayer) to 30 nm (hot yellow) above the substrate. Raised domains dot the landscape and are connected by many thin filaments.⁶⁰

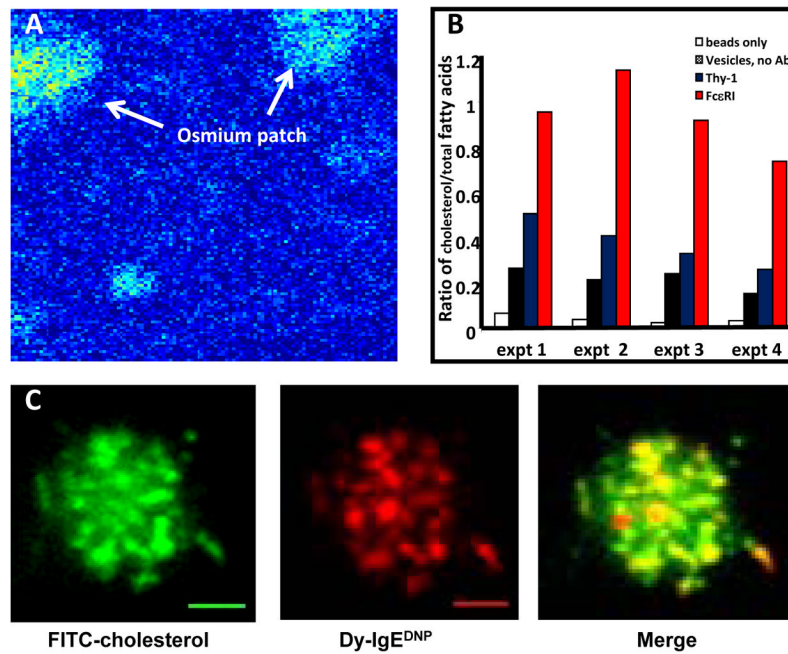


Figure 4.

(A) Pseudo-colored X-ray spectral electron microscopy image, where arrows point to “hot spots” for osmium staining over a region of a membrane sheet. Images were captured on a Phillips FEI Tecnai F30-ST equipped with an EDAX r-TEM SUTW energy dispersive x-ray detector (from ref 75). (B) Results from lipid analysis of IgE-containing vesicles (red) compared to Thy-1-containing vesicles (blue). Lipid content in IgE-vesicles was 50% cholesterol, compared to less than 25% in Thy-1 vesicles. (C) Simultaneous imaging of cholesterol-18 FITC (green) and IgE-FcεRI (red) in the membrane of an RBL cells as it contacts a lipid bilayer containing monovalent DNP. Cholesterol and FcεRI are seen to colocalize in patches that travel together during synapse formation (Carroll-Portillo et al., 2010).